Research Article | Vol. 29, No. 23 / 8 Nov 2021 / Optics Express 37368
Optics EXPRESS

Mechanically stretchable metamaterial with tunable mid-infrared optical properties

FANGQI CHEN,[1] XIAOJIE LIU,[1] YANPEI TIAN,[1] AND YI ZHENG[1,2,*]

[1]Department of Mechanical and Industrial Engineering, Northeastern University, Boston, MA 02115, USA
[2]Department of Electrical and Computer Engineering, Northeastern University, Boston, MA 02115, USA
[*]y.zheng@northeastern.edu

Abstract: Over the past decade, tremendous efforts have been devoted to the design of metamaterials with ultrahigh absorption. These perfect absorbers can realize the annihilation of incident electromagnetic waves by eliminating reflection and transmission of microwaves, infrared, visible, and ultraviolet. However, the optical properties are usually unchanged due to a rigid structure. In this work, we propose a mechanically stretchable metamaterial composed of polydimethylsiloxane and gold with tunable optical properties in the mid-infrared region. A large variation of absorptances with different gold filling ratios is demonstrated as well as the corresponding electric field distributions. Under moderate uniaxial and biaxial tensions, the proposed two-dimensional grating structure has achieved a dynamic tuning of infrared thermal properties, including a sharp reflectance-absorptance switch. This mechanically stretchable metamaterial can serve different optical and sensing functions due to its facile tunability.

1. Introduction

Metamaterials are artificial composite materials with subwavelength structure units and exhibit unique electromagnetic responses via properly tailoring the structural features. Thus, metamaterials demonstrate unique properties that does not exist in natural materials [1–3]. They have been applied in various fields, for example, super-lenses and super-resolution imaging [4–8], negative index materials [9–11], invisibility cloaking [12–14], perfect absorbers [15–18] and so on. Recently, both broadband and narrowband metamaterial absorbers have been proposed over a broad wavelength range covering microwaves, infrared, visible and ultraviolet light [19–25]. Ding et al. experimentally demonstrated broadband, polarization-insensitive and omnidirectional absorbers working in the near-infrared range [26]. The proposed absorber was based on the metal-insulator-metal (MIM) configuration, in which the highly lossy metal titanium contributed to the decrease of the quality factor of the localized surface plasmon resonance, thus leading to the broadband absorption. Tian et al. computationally and experimentally demonstrated a MIM spectrally selective solar absorber. It exhibited high absorptance at solar irradiance wavelength and low emittance at infrared thermal wavelength, which improved the energy conversion efficiency of solar thermal engineering [27].

In addition to the unchanged optical properties, tunable metamaterials have attracted considerable attention in the past few years as well. Based on the phenomenon that causes the change, the tunable metamaterials can be briefly classified into four categories: thermal, optical, mechanical, and electrical tunability [28]. Some active materials are incorporated in the design, such as phase change materials and elastic materials. Chen et al. proposed a tunable plasmonic perfect absorber based on phase change material $Ge_2Sb_2Te_5$ (GST), and a tuning range of 650 nm was achieved by varying the crystallization level of GST [29]. Xu et al. investigated stretchable infrared metamaterials utilizing mechanically flexible and deformable polydimethylsiloxane (PDMS). The tuning ranges of 2.37 μm and 2.36 μm were numerically obtained for ring-shape and cross-shape patterns respectively by stretching along different directions [30]. Over the past decade, great attention has been paid on preparing metamaterials based on flexible polymers, such as PDMS,

#439767 https://doi.org/10.1364/OE.439767
Journal © 2021 Received 5 Aug 2021; revised 6 Oct 2021; accepted 18 Oct 2021; published 27 Oct 2021

Optics EXPRESS

polyimide, polyethylene terephthalate (PET), polyethylene naphthalene (PEN), Kapton, and so on [31–36]. The structural flexibility enables applications on non-planar surfaces and opens a route for wearable electronic devices in a variety of sensor fields [37].

The aforementioned tunable metamaterials mainly focus on the peak shifting for narrowband absorption. In this work, we numerically propose a gold (Au)-PDMS two-dimensional grating structure showing sufficient tuning range in absorptance/reflectance over a broad mid-infrared region from 7 μm to 20 μm. The calculation is based on rigorous coupled wave analysis (RCWA) method. The relationship between the absorptance α and reflectance ρ is $\alpha = 1 - \rho$. The structure is designed to be opaque in the mid-infrared region, therefore, the transmittance is negligible. It is numerically concluded that the absorptance greatly relys on the filling ratio of the Au square patch, especially when it is between 0.8 and 0.92, which is further validated by the electric field distributions. The spectral tuning performance is evaluated under moderate uniaxial (along x or diagonal direction) and biaxial tensions. A sharp reflectance-absorptance switch is realized under a biaxial strain of 0.15.

2. Results and discussion

Figure 1 shows the schematic of the proposed two-dimensional grating structure, which consists of a PDMS substrate and Au square patches on top. The thicknesses of the Au square patch and the PDMS substrate are 50 nm and 700 μm, respectively. The PDMS with thickness of 700 μm is easy to accomplish in a practical experiment. Each Au patch is in a square shape, therefore the side length w_x is equal to w_y. The periods in both x and y directions, Λ_x and Λ_y, are equal to each other in the original state, which can have distinct values when the tensile force is applied to the structure. The original filling ratio $\phi = \phi_x = \phi_y$, here $\phi_x = w_x/\Lambda_x$ and $\phi_y = w_y/\Lambda_y$.

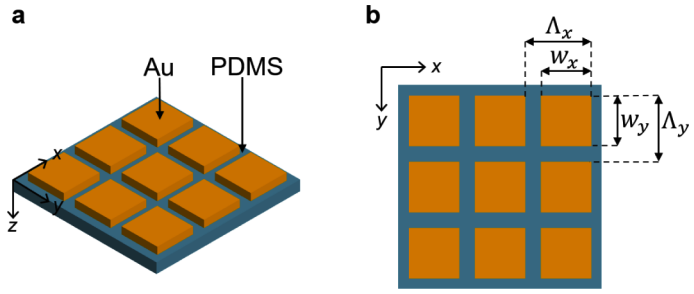

Fig. 1. (a) Schematic of the Au-PDMS two-dimensional grating structure. The thicknesses of the Au square patch and the PDMS substrate are 50 nm and 700 μm, respectively. (b) Top view of the structure. The side lengths of Au square patches, w_x and w_y, are the same. The periods in x and y directions are Λ_x and Λ_y, respectively.

The calculation is performed by RCWA method to study the infrared thermal properties of the proposed reconfigurable metamaterial. The direction of propagation of the incident light is along z direction. The dielectric functions of Au and PDMS can be found in these works [38,39]. The mid-infrared spectrum from 7 μm to 20 μm can be tuned substantially, which greatly depends on the filling ratio ϕ. In Fig. 2(a), both periods Λ_x and Λ_y are fixed at 1 μm. The absorptance is dramatically changed from close-to-unity to nearly zero by increasing the filling ratio. Since PDMS with 700 μm thickness is opaque to the mid-infrared light (Fig. S1), the transmittance of the structure can be negligible. Therefore, the reflectance can also be tuned substantially, but in an opposite trend to the absorptance. It is demonstrated in Fig. 2(a) that the variations of absorptance occur when the filling ratio is larger than 0.8. Therefore, with a small change in filling ratio from 0.8 to 0.92, the structure is switched from high absorptance to high reflectance. In this case, the periods are fixed and different side lengths of the Au square

Optics EXPRESS

patches lead to varying filling ratios accordingly. The tunability can also be realized by changing the periods while the geometry of the Au square patch is fixed (Fig. S2). Since PDMS is an elastomer, it can be easily stretched, thus changing the periods and the filling ratios as well. This provides a convenient way to dynamically manipulate the mid-infrared spectrum by mechanical deformation. In this calculation, the geometric parameters of the Au square patches are assumed to keep unchanged during the stretching process, including the thickness and the side length, as the Young's modulus of Au is much larger than that of PDMS. Moreover, the slight variation of the thickness of the PDMS substrate is neglected for calculation simplicity. The thickness would be thinner when stretched, however, with the strains discussed in the following analysis, the thickness of PDMS is larger than 300 μm, and it is still opaque to the mid-infrared light (Fig. S1). The penetration depth (δ) is calculated via $\delta = \lambda/4\pi\kappa$ [40] and plotted in Fig. 2(b), where λ is the wavelength and κ is the extinction coefficient. It is demonstrated that from 7 μm to 20 μm, the penetration depth of a PDMS bulk is below 80 μm. Thus, it is confirmed that the thickness variation of the PDMS has little impact on the mid-infrared spectra.

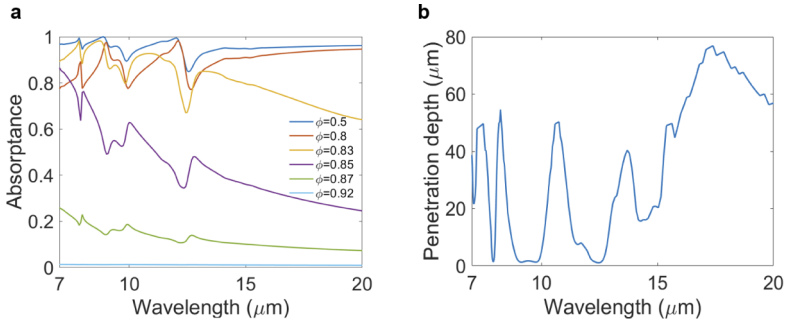

Fig. 2. (a) Absorptance spectra of the structure with varying filling ratios ϕ. Both periods Λ_x and Λ_y are fixed at 1 μm. (b) Penetration depth of a PDMS bulk in the mid-infrared region from 7 μm to 20 μm.

To reveal the physical mechanism of the tunable infrared thermal properties, the electric field $|E_y|$ for TE polarization is plotted at 12 μm, which is in the wavelength region of interest. Figure 3(a) is a schematic of one unit of the proposed structure. The origin of the coordinate system is at the center of the Au top surface. The $y-z$ plane is at $x = 0$, and the $x-y$ plane is at $z = 0.025$ μm. From Figs. 3(b) and 3(d), it is noted that as $\phi = 0.5$, the electric field is strongly confined between adjacent Au square patches along y direction. When ϕ is increased to 0.92 (Figs. 3(c) and 3(e)), this strong confinement almost disappears, and the Au-PDMS structure exhibits high reflectance feature of Au, since the filling ratio now is quite large. The electric field distributions for multiple units are displayed in Fig. S3. To further validate the results, the transmittance spectra of a single Au grating layer and the spectra of a bare PDMS film with thickness of 700 μm are plotted in Fig. S4 and Fig. S5, respectively. The absorptance of the bare PDMS film is close to unity. When the Au filling ratio is as large as 0.8, the transmittance is still higher than 0.8. Thus, the transmitted light is absorbed by the PDMS substrate. As the filling ratio rises to 0.92, there is no transmitted light, and this high-density Au arrays behave as a thin film of Au exhibiting high reflectance.

Next, three common stretching scenarios are discussed. The tensile force is applied only in x direction, in the direction with 45° to the x axis, and in both x and y directions, respectively. When the tensile force is applied only in x direction (Fig. 4(a)), the PDMS is stretched along the x direction and compressed in the y direction. There should be a maximum x-direction strain ε_{xmax} when the PDMS strips between two adjacent Au square patches in y direction totally vanish. The relationship between the original filling ratio ϕ and ε_{xmax} can be derived as $\varepsilon_{xmax} = 2(1-\phi)$.

Optics EXPRESS

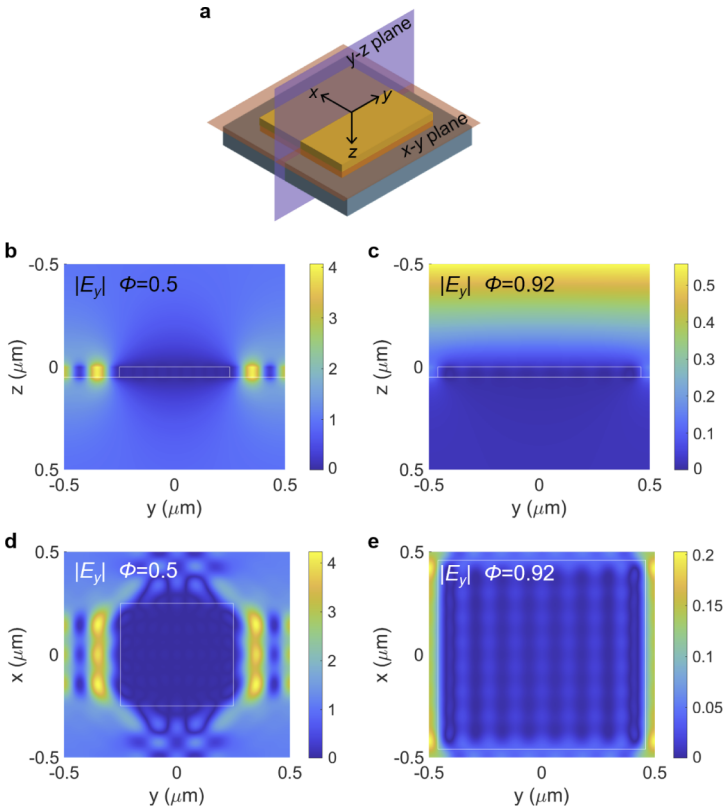

Fig. 3. (a) Schematic of one unit of the Au-PDMS structure. The $y-z$ plane is at $x = 0$. The $x-y$ plane is at $z = 0.025$ μm, and $z = 0$ represents the top surface of the Au layer. The electric field distributions at $y-z$ plane for filling ratios equal to (b) 0.5 and (c) 0.92. The electric field distributions at $x-y$ plane for filling ratios equal to (d) 0.5 and (e) 0.92. The while lines present the side views and top views of the Au grating structure. All electric field distributions are at wavelength of 12 μm.

Based on the results from Fig. 2(a), we focus on the filling ratio ϕ from 0.8 to 0.92, when the dramatic change in the absorptance occurs. Two original states are selected with filling ratios equal to 0.92 and 0.8 for Figs. 4(b) and 4(c), and their respective ε_{xmax} are 0.16 and 0.4. The deformation strain in the y direction ε_y is calculated based on the fact that the Poisson's ratio for PDMS is 0.5. In Fig. 4(b), at the stretched state, ε_x is 0.15, and ε_y equals 0.075. It is shown that the reflectance decreases from close-to-unity at the original state to around 0.5 at the stretched state, and the absorptance increases from near zero to around 0.5. In Fig. 4(c), the original state has high absorptance over 0.8. With a strain of 0.3, both absorptance and reflectance can be tuned to around 0.5.

In Fig. 5(a), when the force is applied in the direction with 45° to the x axis (x' axis), each unit enclosed by red dashed lines is assumed to deform from a square shape to a rhombus, while the Au square patches are still in the center of each unit. A new $x'-y'$ coordinate and a new unit with blue dashed lines are introduced here. The blue unit still remains a rectangular shape upon stretching, which helps us to build the model in RCWA calculation and perform the analysis. The limiting case happens when adjacent vertexes of the Au square patches contact in the y' direction. The relationship between the original filling ratio ϕ and $\varepsilon_{x'max}$ can be derived as $\varepsilon_{x'max} = 2(1-\phi)$. The original filling ratios for Fig. 5(b) and (c) are 0.92 and 0.85, respectively. Therefore, $\varepsilon_{x'max}$

Optics EXPRESS

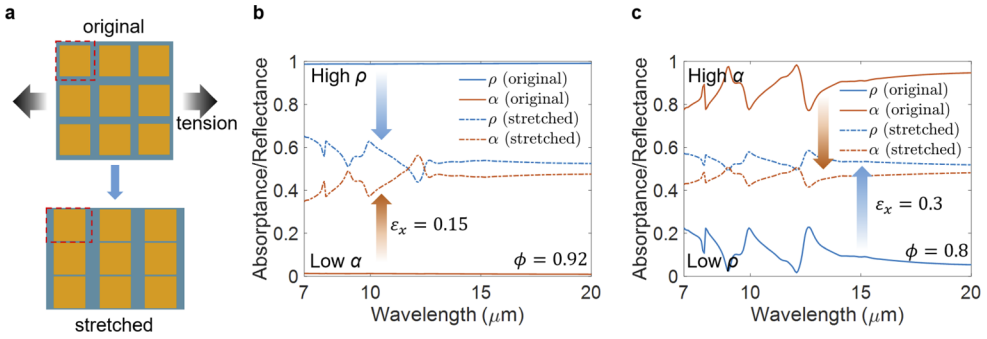

Fig. 4. (a) The deformation process when the tensile force is applied in x direction. (b)(c) Absorptance α and reflectance ρ from 7 μm to 20 μm as the structure is in the original or stretched state. The original filling ratios for (b) and (c) are 0.92 and 0.8, respectively. The strains in x direction for stretched states in (b) and (c) are 0.15 and 0.3, respectively.

are 0.16 and 0.3, respectively. Similar variation trends are observed for both absorptance and reflectance as compared with the results in Fig. 4. The structures show high reflectance (Fig. 5(b)) and high absorptance (Fig. 5(c)) at their original states, while the reflectance and absorptance become closer to each other at the stretched states.

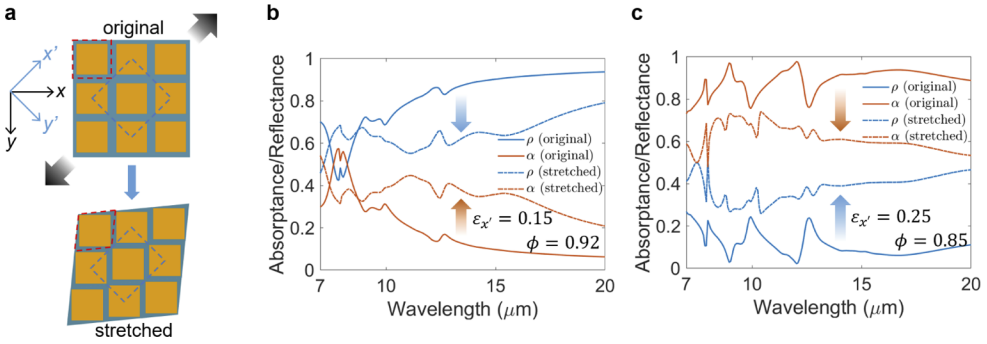

Fig. 5. (a) The deformation process when the tensile force is applied in the direction with 45° to the x axis (x' axis). (b)(c) Absorptance α and reflectance ρ from 7 μm to 20 μm as the structure is in the original or stretched state. The original filling ratios for (b) and (c) are 0.92 and 0.85, respectively. The strains in x' direction for stretched states in (b) and (c) are 0.15 and 0.25, respectively.

Based on the aforementioned two stretching scenarios, a quite large tuning range has been achieved for absorptance and reflectance. Furthermore, it is possible to make this tuning range even larger, for example, from high reflectance to low reflectance (high absorptance). Based on the relationship between the absorptance and the filling ratios in Fig. 2(a), this reflectance-absorptance switch can only be achieved when both ϕ_x and ϕ_y increase or decrease simultaneously. Therefore, in Fig. 6(a), the tensile forces are applied in both x and y directions. The original filling ratio of the structure is 0.92, when it shows a high reflectance feature (Fig. 6(b)). Upon stretching to $\varepsilon_x = \varepsilon_y = 0.15$, the structure switches to a high absorptance, while the reflectance is mainly below 0.2 in the mid-infrared region from 7 μm to 20 μm. Same stretched state can be obtained as the tensile forces are applied in the diagonal directions (the orange arrows). In summary, with only a small biaxial strain of 0.15, the optical characteristics can be totally reversed. Moreover, reflectance spectra at various incident angles of 15°, 30°, 45° and 60° are investigated. Figure

Optics EXPRESS

S6a, b and c demonstrate the unstretched state, uniaxially stretched state in x direction and biaxially stretched state, respectively. The original filling ratios for these three cases are all equal to 0.92. In all three cases, the reflectance of the Au-PDMS structure varies under different incident angles. However, the changes are not magnificent. Combined with the corresponding normal incidence results in Fig. 4(b) and Fig. 6, this structure exhibits an angle-independent characteristic with incident angles up to 60°.

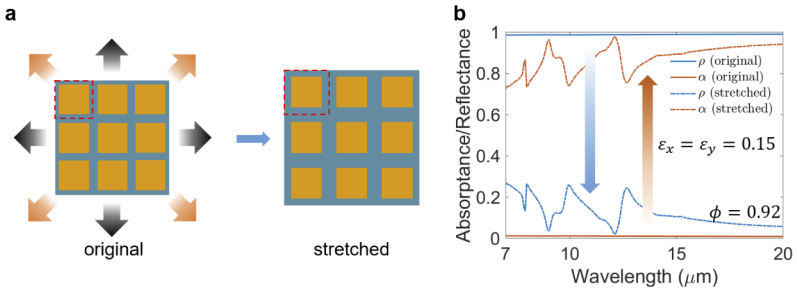

Fig. 6. (a) The deformation process when the tensile forces are applied biaxially. (b) Absorptance α and reflectance ρ from 7 μm to 20 μm as the structure is in the original or stretched state. The original filling ratio is 0.92. The strains in x and y directions for stretched states are both 0.15.

3. Conclusion

Metamaterials exhibiting extraordinary properties that cannot be found in nature have aroused tremendous attention over the past decade, such as negative index materials, invisibility cloaking and perfect absorbers. To increase the flexibility of metamaterials, there are literatures reporting the tuning mechanisms, for example, semiconductor diodes, ferroelectric materials and liquid crystals. Herein, a reconfigurable and stretchable metamaterial composed of two-dimensional Au gratings and PDMS substrate is reported. Easily tunable absorptance and reflectance in the mid-infrared region from 7 μm to 20 μm is presented under controllable mechanical deformation, especially when the filling ratio is in a small range between 0.8 and 0.92. The electric field distributions with distinct filling ratios are shown to better understand the physical mechanism of the tunable infrared thermal properties. Two uniaxial and one biaxial stretching scenarios are investigated, all of which exhibit an outstanding spectral tuning capability. Therein, the biaxial stretching scenario shows the largest tuning range and achieves a sharp reflectance-absorptance switch. Furthermore, the simplistic tunable approach employed herein may be easily applied to other soft materials and geometries to further enhance tunability.

Funding. National Science Foundation (CBET-1941743).

Disclosures. The authors declare no conflicts of interest.

Data availability. Data underlying the results presented in this paper are not publicly available at this time but may be obtained from the authors upon reasonable request.

Supplemental document. See Supplement 1 for supporting content.

References

1. Y.-S. Lin, C.-Y. Huang, and C. Lee, "Reconfiguration of resonance characteristics for terahertz u-shape metamaterial using mems mechanism," IEEE J. Sel. Top. Quantum Electron. **21**(4), 93–99 (2015).
2. D. Hasan and C. Lee, "Hybrid metamaterial absorber platform for sensing of co2 gas at mid-ir," Adv. Sci. **5**(5), 1700581 (2018).
3. V. G. Veselago, "Electrodynamics of substances with simultaneously negative values of ε and μ," Usp. Fiz. Nauk **92**(7), 517 (1967).

Optics EXPRESS

4. M. Kim, S. So, K. Yao, Y. Liu, and J. Rho, "Deep sub-wavelength nanofocusing of uv-visible light by hyperbolic metamaterials," Sci. Rep. **6**(1), 38645 (2016).
5. Z. Liu, H. Lee, Y. Xiong, C. Sun, and X. Zhang, "Far-field optical hyperlens magnifying sub-diffraction-limited objects," Science **315**(5819), 1686 (2007).
6. D. Lee, Y. D. Kim, M. Kim, S. So, H.-J. Choi, J. Mun, D. M. Nguyen, T. Badloe, J. G. Ok, K. Kim, H. Lee, and J. Rho, "Realization of wafer-scale hyperlens device for sub-diffractional biomolecular imaging," ACS Photonics **5**(7), 2549–2554 (2018).
7. J. Rho, Z. Ye, Y. Xiong, X. Yin, Z. Liu, H. Choi, G. Bartal, and X. Zhang, "Spherical hyperlens for two-dimensional sub-diffractional imaging at visible frequencies," Nat. Commun. **1**(1), 143 (2010).
8. Z. Jacob, L. V. Alekseyev, and E. Narimanov, "Optical hyperlens: far-field imaging beyond the diffraction limit," Opt. Express **14**(18), 8247–8256 (2006).
9. D. R. Smith, W. J. Padilla, D. Vier, S. C. Nemat-Nasser, and S. Schultz, "Composite medium with simultaneously negative permeability and permittivity," Phys. Rev. Lett. **84**(18), 4184–4187 (2000).
10. D. R. Smith, J. B. Pendry, and M. C. Wiltshire, "Metamaterials and negative refractive index," Science **305**(5685), 788–792 (2004).
11. J. Valentine, S. Zhang, T. Zentgraf, E. Ulin-Avila, D. A. Genov, G. Bartal, and X. Zhang, "Three-dimensional optical metamaterial with a negative refractive index," Nature **455**(7211), 376–379 (2008).
12. U. Leonhardt and T. Tyc, "Broadband invisibility by non-euclidean cloaking," Science **323**(5910), 110–112 (2009).
13. D. Schurig, J. J. Mock, B. Justice, S. A. Cummer, J. B. Pendry, A. F. Starr, and D. R. Smith, "Metamaterial electromagnetic cloak at microwave frequencies," Science **314**(5801), 977–980 (2006).
14. W. Cai, U. K. Chettiar, A. V. Kildishev, and V. M. Shalaev, "Optical cloaking with metamaterials," Nat. Photonics **1**(4), 224–227 (2007).
15. D. M. Nguyen, D. Lee, and J. Rho, "Control of light absorbance using plasmonic grating based perfect absorber at visible and near-infrared wavelengths," Sci. Rep. **7**(1), 1–8 (2017).
16. T. Badloe, J. Mun, and J. Rho, "Metasurfaces-based absorption and reflection control: perfect absorbers and reflectors," J. Nanomater. **2017**, 1–18 (2017).
17. N. I. Landy, S. Sajuyigbe, J. J. Mock, D. R. Smith, and W. J. Padilla, "Perfect metamaterial absorber," Phys. Rev. Lett. **100**(20), 207402 (2008).
18. I. Kim, S. So, A. S. Rana, M. Q. Mehmood, and J. Rho, "Thermally robust ring-shaped chromium perfect absorber of visible light," Nanophotonics **7**(11), 1827–1833 (2018).
19. B. Wang, T. Koschny, and C. M. Soukoulis, "Wide-angle and polarization-independent chiral metamaterial absorber," Phys. Rev. B **80**(3), 033108 (2009).
20. Z. H. Jiang, S. Yun, F. Toor, D. H. Werner, and T. S. Mayer, "Conformal dual-band near-perfectly absorbing mid-infrared metamaterial coating," ACS Nano **5**(6), 4641–4647 (2011).
21. Y. Cui, J. Xu, K. Hung Fung, Y. Jin, A. Kumar, S. He, and N. X. Fang, "A thin film broadband absorber based on multi-sized nanoantennas," Appl. Phys. Lett. **99**(25), 253101 (2011).
22. M. K. Hedayati, M. Javaherirahim, B. Mozooni, R. Abdelaziz, A. Tavassolizadeh, V. S. K. Chakravadhanula, V. Zaporojtchenko, T. Strunkus, F. Faupel, and M. Elbahri, "Design of a perfect black absorber at visible frequencies using plasmonic metamaterials," Adv. Mater. **23**(45), 5410–5414 (2011).
23. Z. Fang, Y.-R. Zhen, L. Fan, X. Zhu, and P. Nordlander, "Tunable wide-angle plasmonic perfect absorber at visible frequencies," Phys. Rev. B **85**(24), 245401 (2012).
24. N. Landy, C. Bingham, T. Tyler, N. Jokerst, D. Smith, and W. Padilla, "Design, theory, and measurement of a polarization-insensitive absorber for terahertz imaging," Phys. Rev. B **79**(12), 125104 (2009).
25. J. Zhu, S. Yan, N. Feng, L. Ye, J.-Y. Ou, and Q. H. Liu, "Near unity ultraviolet absorption in graphene without patterning," Appl. Phys. Lett. **112**(15), 153106 (2018).
26. F. Ding, J. Dai, Y. Chen, J. Zhu, Y. Jin, and S. I. Bozhevolnyi, "Broadband near-infrared metamaterial absorbers utilizing highly lossy metals," Sci. Rep. **6**(1), 39445 (2016).
27. Y. Tian, X. Liu, A. Ghanekar, and Y. Zheng, "Scalable-manufactured metal–insulator–metal based selective solar absorbers with excellent high-temperature insensitivity," Appl. Energy **281**, 116055 (2021).
28. S. Bang, J. Kim, G. Yoon, T. Tanaka, and J. Rho, "Recent advances in tunable and reconfigurable metamaterials," Micromachines **9**(11), 560 (2018).
29. Y. Chen, X. Li, X. Luo, S. A. Maier, and M. Hong, "Tunable near-infrared plasmonic perfect absorber based on phase-change materials," Photonics Res. **3**(3), 54–57 (2015).
30. R. Xu, J. Luo, J. Sha, J. Zhong, Z. Xu, Y. Tong, and Y.-S. Lin, "Stretchable ir metamaterial with ultra-narrowband perfect absorption," Appl. Phys. Lett. **113**(10), 101907 (2018).
31. S. Walia, C. M. Shah, P. Gutruf, H. Nili, D. R. Chowdhury, W. Withayachumnankul, M. Bhaskaran, and S. Sriram, "Flexible metasurfaces and metamaterials: A review of materials and fabrication processes at micro-and nano-scales," Appl. Phys. Rev. **2**(1), 011303 (2015).
32. I. M. Pryce, K. Aydin, Y. A. Kelaita, R. M. Briggs, and H. A. Atwater, "Highly strained compliant optical metamaterials with large frequency tunability," Nano Lett. **10**(10), 4222–4227 (2010).
33. T. Jang, H. Youn, Y. J. Shin, and L. J. Guo, "Transparent and flexible polarization-independent microwave broadband absorber," ACS Photonics **1**(3), 279–284 (2014).

Optics EXPRESS

34. Y. Shan, L. Chen, C. Shi, Z. Cheng, X. Zang, B. Xu, and Y. Zhu, "Ultrathin flexible dual band terahertz absorber," Opt. Commun. **350**, 63–70 (2015).
35. P. K. Singh, K. A. Korolev, M. N. Afsar, and S. Sonkusale, "Single and dual band 77/95/110 ghz metamaterial absorbers on flexible polyimide substrate," Appl. Phys. Lett. **99**(26), 264101 (2011).
36. X. Chen and W. Fan, "Ultra-flexible polarization-insensitive multiband terahertz metamaterial absorber," Appl. Opt. **54**(9), 2376–2382 (2015).
37. S. Aksu, M. Huang, A. Artar, A. A. Yanik, S. Selvarasah, M. R. Dokmeci, and H. Altug, "Flexible plasmonics on unconventional and nonplanar substrates," Adv. Mater. **23**(38), 4422–4430 (2011).
38. R. L. Olmon, B. Slovick, T. W. Johnson, D. Shelton, S.-H. Oh, G. D. Boreman, and M. B. Raschke, "Optical dielectric function of gold," Phys. Rev. B **86**(23), 235147 (2012).
39. M. R. Querry, *Optical constants of minerals and other materials from the millimeter to the ultraviolet* (Chemical Research, Development & Engineering Center, US Army Armament . . . , 1987).
40. M. F. Modest, *Radiative heat transfer* (Academic press, 2013).